

---

[All ETDs from UAB](#)

[UAB Theses & Dissertations](#)

---

2010

## **Fabrication and Dynamic Mechanical Analysis of Hydroxyapatite Nanoparticle /Gelatin Porous Scaffolds**

Hicham K. Ghossein  
*University of Alabama at Birmingham*

Follow this and additional works at: <https://digitalcommons.library.uab.edu/etd-collection>

---

### **Recommended Citation**

Ghossein, Hicham K., "Fabrication and Dynamic Mechanical Analysis of Hydroxyapatite Nanoparticle /Gelatin Porous Scaffolds" (2010). *All ETDs from UAB*. 1735.  
<https://digitalcommons.library.uab.edu/etd-collection/1735>

This content has been accepted for inclusion by an authorized administrator of the UAB Digital Commons, and is provided as a free open access item. All inquiries regarding this item or the UAB Digital Commons should be directed to the [UAB Libraries Office of Scholarly Communication](#).

Fabrication and Dynamic Mechanical Analysis of Hydroxyapatite Nanoparticle /Gelatin Porous  
Scaffolds

by

HICHAM GHOSSEIN

ANDREI STANISHEVSKY, COMMITTEE CHAIR  
YOGESH VOHRA  
SERGEY VYAZOVKIN

A THESIS

Submitted to the graduate faculty of The University of Alabama at Birmingham,  
in partial fulfillment of the requirements for the degree of  
Master of Science

BIRMINGHAM, ALABAMA

2010

Copyright by  
Hicham Ghossein  
2010

# **Fabrication and Dynamic Mechanical Analysis of Hydroxyapatite Nanoparticle /Gelatin Porous Scaffolds**

HICHAM GHOSSEIN

UAB Department of Physics

## **ABSTRACT**

The application of engineered biomaterial scaffolds for hard tissue repair critically depends on the scaffold's internal architecture at various length scales. The pore size, shape, surface morphology, and pore connectivity are among the most important factors that affect the scaffold's mechanical properties and biointegration.

Reported in this thesis are the results of the investigation of porous constructs fabricated by a freeze-drying process from synthetic nanosized hydroxyapatite / gelatin (nanoHA/Gel) dispersions with different nanoHA/Gel ratios (nanoHA loading was varied from 0 to 50 % by weight). The fabricated scaffolds had porosity up to 90% with pore size in the range of 100 - 500  $\mu\text{m}$ , and good distribution of HA nanoparticles within the gelatin matrix. Such porosity is considered to be close to optimal to promote a good cell adhesion in the potential applications of prepared constructs.

The fabricated scaffolds have been investigated using X-ray diffraction (XRD), Fourier-Transform Infrared Spectroscopy (FTIR), and Dynamic

Mechanical Analysis (DMA). Dynamic mechanical analysis of as-fabricated scaffolds revealed that the scaffolds achieved maximum bending and tensile moduli up to 1.28 GPa and 1.5 GPa, respectively, when nanoHA loading was around 30 % by weight. The bending modulus increases by a factor of 1.6, while the Tension modulus increased by a factor of 0.8 after the cross-linking of polymer. Higher nanoHA loading above 50 % by weight results in bending modulus of about 700 MPa and Tension modulus of about 200 MPa only. However, the cross-linking still enhanced the bending up to 1 GPa while it did not affect much the Tension modulus in 50% nanoHA/gelatin constructs.

It has been shown that the cross-linking with glutaraldehyde solution improves the morphological structure of the scaffolds, while there was no apparent effect of the cross-linking on the chemical changes in both organic and inorganic content during the processing.

The results of this study can be useful for further development of nanoparticulate bioceramic / biopolymer constructs for applications in biomedical field.

Keywords: Gelatin, Nano HA, Mechanical, Morphological, Modulus, Crosslinking.

## ACKNOWLEDGEMENTS

First, I would like to thank my advisor, Dr. Stanishevsky for all his support and guidance in understanding this research. He was the good example of a professional researcher and scientist. Without his help the path of performing a good scientific research would be much harder, and much confusing.

I would also like to thank my committee members Dr. Vohra and Dr. Vyazovkin for their professional response and help, even within a short notice from me. I understand the load of work that they carry, thus they were there for me when I needed their help.

I want also to thank all those who helped me in my research. Dr. Ion Daranka for the time he spends teaching me how to operate the DMA machine, and to understand the way it works. MR. Michael Walock for showing me how to work with the SEM. Miss Yujao Zou and Dr. Gopi Samudrala for their help with the XRD.

And a special appreciation and thanks for my family, especially my parents. Who have supported me in all possible way, they lift me up when I fell under the pressure. They gave me the strength to carry on the road. And most important they taught me how to achieve the impossible. They are the giants that gave me their shoulders so I can reach higher.

Least but not last, UAB Physics Department faculty, staff, and grad students, for all their efforts in sharing knowledge with me so I can become a better physicist and a real man of science; for their ethics and support, and most

important for believing in me and in my potentials. They all made my experience in UAB unforgettable.

Also, I would like to mention that this study was partially supported by the National Science Foundation (Award Number CMS-0555778). And the FTIR micro-spectroscopy facility used in the analysis of the samples was supported by the National Institutes of Health - National Center for Research Resources (Award Number S10RR023388).

## TABLE OF CONTENTS

	<i>Page</i>
ABSTRACT.....	iii
ACKNOWLEDGEMENTS.....	v
LIST OF TABLES.....	viii
LIST OF FIGURES.....	ix
CHAPTER	
1 BACKGROUND AND MOTIVATION.....	1
A. Introduction.....	1
B. Background.....	5
2 EXPERIMENTAL METHODS.....	12
A. Fabrication of scaffolds.....	12
B. Methods of investigation.....	14
i. Structural investigation.....	14
ii. Mechanical testing.....	15
3 RESULTS AND DISCUSSION.....	17
A. SEM results.....	17
i. Sample 1: 10% HA by weight.....	18
ii. Sample 2: 30% HA by weight.....	19
iii. Sample 3: 50% HA by weight.....	20
B. XRD measurements.....	21
C. Infrared spectroscopy.....	23
D. Mechanical testing.....	25
CONCLUSIONS.....	36
LIST OF REFERENCES.....	37

LIST OF TABLES

<i>Table</i>	<i>Page</i>
1 Elastic Modulus measured From Compressive Stress-Strain Curves within Initial Stage (<2% Strain) <sup>a</sup> .....	10

## LIST OF FIGURES

<i>Figure</i>	<i>Page</i>
1 Manufacture of bioactive composite scaffolds .....	6
2 CHA/PHBV composite scaffold produced through an emulsion freeze-drying process .....	7
3 The TEM photograph of n-HA/CS/CMC composite.....	9
4 The SEM microstructure of n-HA/CS/CMC composite scaffold. ....	9
5 Schematic of synthesis of HA/Gel Scaffolds.....	13
6 Test assembly for Mechanical testing.....	16
7 Test sample for SEM images and the areas where the picture were taken.....	18
8 SEM pictures for Sample 1 that contain 10 wt % HA. ....	19
9 SEM pictures for Sample 2 that contain 30 wt % HA. ....	20
10 SEM pictures for Sample 3 that contain 50 wt % HA. ....	21
11 XRD patterns of the gelatin and gelatin-HA composite foams .....	22
12 IR spectra for gelatin sample, and all other samples before Crosslinking.....	24
13 IR spectra for gelatin sample, and all other samples after Crosslinking.....	25

<i>Figure</i>	<i>Page</i>
14 Comparison for bending modulus between all old samples before crosslinking.....	27
15 Comparison for tension modulus between all old samples before crosslinking.....	28
16 Comparison for bending modulus between all old samples after crosslinking .....	29
17 Comparison for tension modulus between all old samples after crosslinking.....	30
18 Comparison between the Bending Modulus of all new samples before Crosslinking.....	31
19 Comparison between the Tension Modulus of all new samples before Crosslinking.....	32
20 Comparison between the Bending Modulus of all new samples after Crosslinking.....	33
21 Comparison between the Tension Modulus of all new samples after Crosslinking.....	34

## CHAPTER 1

### BACKGROUND AND MOTIVATION

#### A. Introduction

Since the late 1980's tissue engineering (TE) as a new discipline has made rapid advances. Tissue engineering, as a potential medical treatment, holds promises of eliminating re-operations by using biological substitutes, solving problems of implant rejection, transmission of diseases associated with xenografts and allografts, and shortage in organ donation, and potentially offering treatments for medical conditions that are currently untreatable [1]. Such a treatment hold as well a strong economical strength, due to its low cost in comparing to the available treatments these days Since, at the present, it is estimated that approximately one seventh of the US population suffers from musculoskeletal impairment, costing the US economy more than \$215 billion a year. Well over 600,000 orthopedic surgical procedures performed annually in the US would require bone grafts. With a growing and aging population, this number will continue to increase [2]. Not mentioning osteoporosis and other bone problems and diseases that have been a great concern in the last era. Disease statistics from the National Osteoporosis Foundation bear out the magnitude of the problem: One in two women and one in four men over the age of 50 will suffer an osteoporosis-related fracture over their remaining lifetimes [3]. But, even to date, autograft and allograft treatments for bone loss have achieved varying degrees of success in restoring form and function; they still carry significant risks [4]. That is why there are currently many efforts to reduce and eliminate

those risks especially with the large number of people who suffer from osteo-related problem.

One of the possible solutions to achieve this reduction or eliminating the risks is making an alternative synthetic scaffold that is biocompatible, osteoconductive and able to withstand mechanical loading. Thus, creating materials with composition, structure, and properties that are similar to those of human bone is critical for designing artificial bone replacements and curing such diseases as osteoporosis and other related bones problems.

For bone tissue engineering, major issues of tissue engineering scaffolds include the use of appropriate matrix materials for scaffolds, control of porosity and pore characteristics of scaffolds, mechanical strength of scaffolds, scaffold degradation properties, and bioactivity. Compared to the strengths of metals and ceramics for medical applications, the strengths of biodegradable polymers are already very low [1]. On one Hand, gelatin as natural polymer, being a denatured form of collagen, is expected to be beneficial in it for hard tissue applications, because it contains a bunch of biological functional groups, such as amino acids within the backbone. However, the mechanical properties of gelatin are not satisfactory for hard tissue engineering.[5] And a problem has been rising with the introduction of pores into the polymer materials to form tissue engineering scaffolds; the strengths of porous structures are further decreased, as strengths of materials decrease drastically with an increase in porosity [6].On the other hand, some promising polymers such as PLA and poly(e-caprolactone) (PCL) are considered to be non-osteoconductive, and they are cannot be readily biointegrated in hard tissue repair. In order to design better scaffolds for bone tissue engineering, a

composite strategy should therefore be adopted, for example, through the utilization of bioceramic and polymer composite materials [7]. Polymer-based scaffolds containing bioactive bioceramics can be manufactured in such way where the bioceramics can serve two purposes: (a) making the scaffolds osteoconductive, and (b) reinforcing the scaffolds [1].

In a number of published studies, the particulate materials such as hydroxyapatite (HA), tricalcium phosphate (TCP) and a few bioactive glasses have been used in composite scaffolds for achieving osteoconductivity. [6] HA ceramic, being similar to bone mineral in physicochemical properties, is well known for its bioactivity and osteoconductivity in vitro and in vivo [8][9][3]. However, pure HA ceramic scaffolds are difficult to handle and keep in defect sites of the bone because of its brittleness and low plasticity [10]. However, the brittleness of porous ceramic materials and their tendency to form debris can be reduced by adding a polymer. Gelatin is a natural polymer that has been shown to be useful, by Tamperi A et al [11] and Liu B et al [12], as a reinforcing coat for porous cellular isotropic scaffolds, and it also exhibits several biologically attractive features. [13]

So, among the biomaterials proposed, the composites of HA and natural polymers (collagen and gelatin) have a great potential due to their compositional similarity to the physiochemical properties of the human bone [14][15].

Currently, there are a number of strategies for developing bone tissue engineering scaffolds. The composite strategy provides the means for achieving stronger and bioactive scaffolds as compared to conventional polymer scaffolds. Different approaches in the composite fabrication result in scaffolds of different, distinctive characteristics.[1]

From many techniques that have been used for scaffold design, solvent casting/particulate leaching (SCPL), thermally induced phase separation (TIPS), microsphere sintered known as electrospinning, and hydrogel [<sup>16, 17, 18, 19, 20, 21, 22, 23</sup> and <sup>24</sup>] have been shown to be successful. Alternatively, electrospinning technique is an attractive method to fabricate scaffolds. For example, the electro-spinning process was used to make the constructs where the activated polymer chains intertwine with neighboring polymer chains, which finally formed bonding between neighboring microspheres of the sintered gel matrix [<sup>25</sup>]. In Min Wang paper [<sup>1</sup>], it has been found that all electrospinning parameters (polymer solution concentration, solution feeding rate, injection needle diameter, electrical voltage, and working distance) all had significant effects on the resultant fibers. But real form porosity was never properly achieved, in another word good the pore size was not sufficient for in vivo cell infiltration and interconnectivity would fail due to some closed pores. Another process called freeze-drying have been used to develop scaffolds with aligned channel-like meso- and macropores and good micro-interconnections.[<sup>26</sup>] In the sited study [<sup>25</sup>] the gelatin-HA composites were fabricated as a foam, through a novel mixing, freeze-drying, and crosslinking process, to offer the system a high specific surface area for vascularization and cell ingrowth. It has been shown that the freeze-drying method resulted in good porosity. That is why the present study has been focused on the fabrication of the composite porous ceramic/polymer materials using new approaches for mixing, freeze-drying, and crosslinking processes. During the course of present investigation, different HA nanoparticle / gelatin mixtures with different resulting porosity and different nanoHA/Gel ratios (nanoHA loading was varied from 0 to 50 % by weight in preliminary work) have been prepared to optimize the process parameters, to

analyze and understand better the mechanical performance of such constructs, for designing biomedical scaffolds with better performance.

There have been two different approaches to ‘explaining’ the mechanical properties of bone. One approach is to explain the mechanical properties by reference to the microscopic and fine structure of the bone. The other approach is to relate statistically the mechanical behavior to other features of the bone, such as porosity, the general orientation of the bone’s structure or the mineral content. This is phenomenological: one can explain mechanical properties in terms of other variables and use such relationships for prediction. The properties mainly examined were the Young’s modulus and those associated with tensile failure.<sup>[27]</sup> In the present study, this approach was used to explain and analyze the mechanical properties of the fabricated scaffolds in terms of other variables like the weight % of the inorganic phase and use such relationships for prediction on how to make a better scaffold.

#### B. Background:

As mentioned in the Introduction, there are different approaches for the fabrication and for the testing of the ceramic/polymer composite materials. And even more approaches to explain the mechanical properties of the system. Especially, that Bone tissue engineering is a hot and important topic in the scientific community these days. In our study we considered the fabrication by freeze-drying method for bones scaffolds, and we will analyze the mineral content of the scaffold to relate it to its mechanical properties.

For example, in the investigation done by M. Wang in his paper “Composite Scaffolds for Bone Tissue Engineering”, plasma sprayed HA particles (psHA) were

incorporated in a poly(L-lactic acid) (PLLA) to form osteoconductive composite scaffolds [28]. The manufacturing process of these scaffolds is shown in Fig.1.

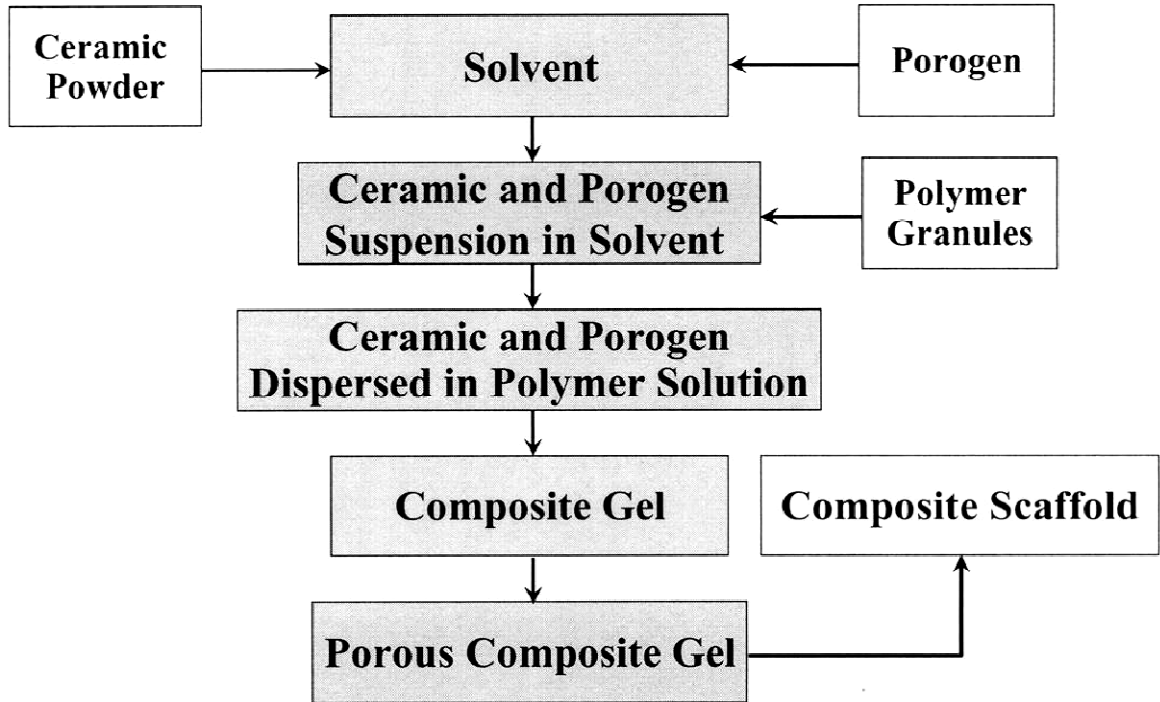


Figure 1: Manufacture of bioactive composite scaffolds[28]

In this process, freeze-drying was used at the final stage to produce the porous structure. Just as in the production of polymer scaffolds [29], for composite scaffolds, factors such as polymer solution concentration, porogen type and size, freeze-drying parameters, etc. play very important roles in forming the scaffolds of desired porous structures (pore geometry, pore size and size distribution, pore interconnectivity, thickness of pore walls, etc.) and hence in the scaffold's mechanical performance. It has been shown through *in vitro* experiments that the composite scaffolds possessed bioactivity due to the incorporation of psHA particles. [1]

In another recent study, it has been shown that using an emulsion freeze-drying process, composite scaffolds based on natural polymers could be produced [30]. In these scaffolds, the carbonated HA (CHA) nanospheres were incorporated. Through this process, highly porous structure with a controlled pore morphologies could be achieved (Fig.2).

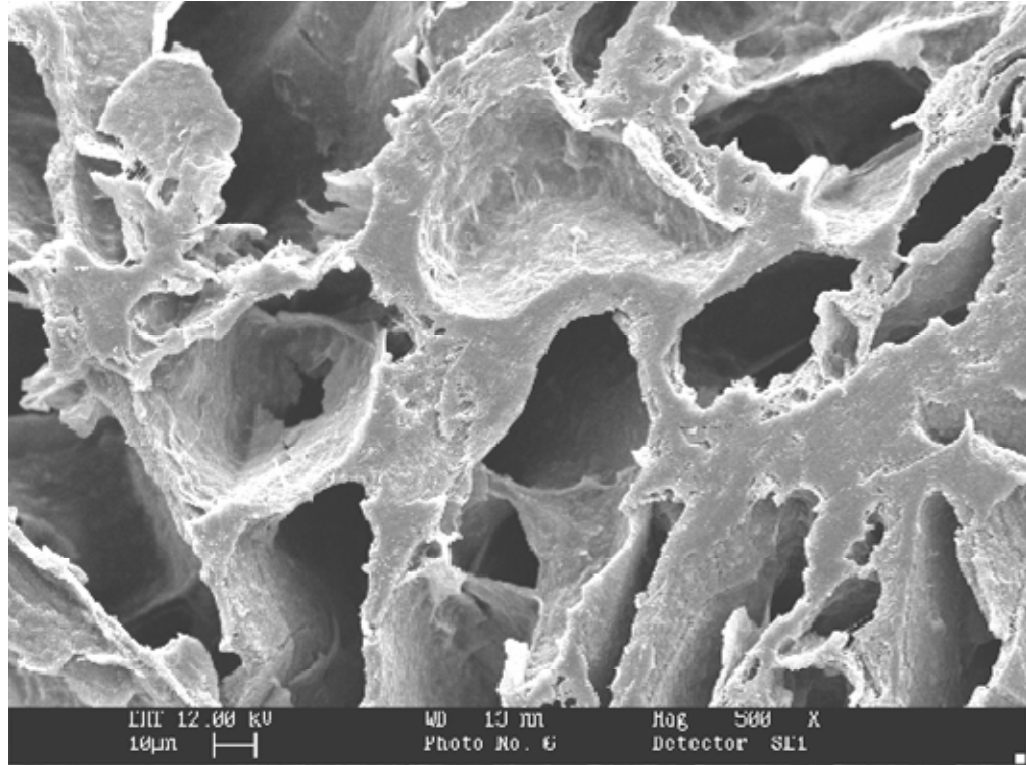


Fig. 2: CHA/PHBV composite scaffold produced through an emulsion freeze-drying process [1]

In another study done by J. Liuyun, et al [31], the nano-hydroxyapatite and natural derived polymers of chitosan and carboxymethyl cellulose, namely, n-HA/CS/CMC scaffold was fabricated as described by the following procedure. Firstly, 3 g CS and 3 g CMC powders were mixed evenly and added into 150 ml n-HA slurry(containing 4 g n-HA powder) with constant stirring for 2 hours under ambient conditions to obtain a homogeneous mixture. Secondly, 3 ml glacial acetic acid was added, and the stirring was

kept till solidified mixture was obtained. Then the solidified mixture was maintained in a freezer at  $-30^{\circ}\text{C}$  for overnight to freeze the solvent. Finally the sample was lyophilized in a freezing dryer until dried, and a scaffold was achieved. To remove the residue acetic acid, the scaffold was immersed in  $0.2 \text{ mol/l NaOH}$  solution for several hours, and then washed in deionized water and dried in a vacuum oven at  $60^{\circ}\text{C}$ .

In order to illustrate intermolecular interaction between components in system, IR spectroscopy measurements were taken. However, an absorption at  $1655 \text{ cm}^{-1}$  in CS were shifted to  $1621 \text{ cm}^{-1}$  in n-HA/CS/CMC composite scaffold, and the peak of  $-\text{NH}_2$  ( $1599 \text{ cm}^{-1}$ ) was absent, which may be the result of the formation of  $-\text{NH}_3^+$ , and the peak of asymmetry stretching of  $-\text{COO}^-$  is still found at  $\sim 1420 \text{ cm}^{-1}$ . Obviously, these observations mean that there was electrostatic attraction between  $-\text{NH}_3^+$  of CS and  $-\text{COO}^-$  of CMC, which results in the formation of CS/CMC polyelectrolyte network, and n-HA was filled in it easily.

Additionally, TEM photograph of the n-HA/CS/CMC composite was given (Fig. 3). It shows that n-HA crystals are still in the range of nanometer grade and have a good dispersive property in the polymers, which has a positive effect on the mechanical and biological properties of the n-HA/CS/CMC composite scaffold.

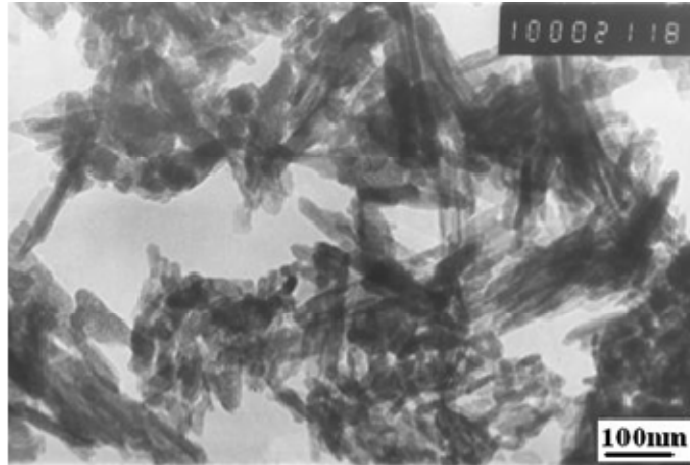


Figure 3: The TEM photograph of n-HA/CS/CMC composite.

The SEM images (Fig. 4) showed that the scaffold was three-dimensional complicated irregular porous structure together with good interconnections between the pores (Fig. 4(a) and 4(b)), and the walls of the macropores ranging about from 100 to 500  $\mu\text{m}$  contained many micropores (Fig. 4(c)).

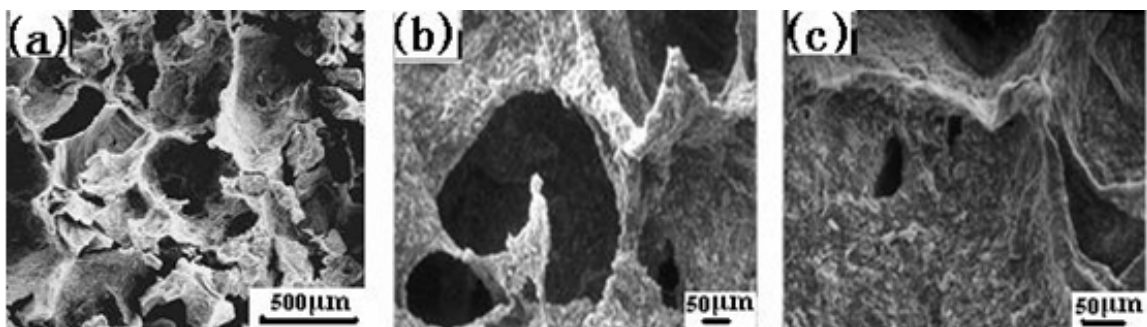


Figure 4: The SEM microstructure of n-HA/CS/CMC composite scaffold.

In addition, the porosity was  $77.8\% \pm 3.24$ . More important, the compressive strength of the scaffold could also reach  $3.5 \pm 0.13$  MPa, which was within the range of the observed properties of cancellous bone (2MPa~10 MPa). Based on the highly porous

structure, it was proposed that it was likely for the scaffold to promote cell adhesion and attachment as well as nutrient delivery to the site of tissue regeneration.

The mechanical properties of the gelatin and gelatin–HA were also tested in their dry and wet state by H.-W.Kim, J. C. Knowles, and H.-E. Kim [<sup>28</sup>]. The results showed that for the dry state the elastic modulus was 0.86 MPa for the pure Gelatin, 2.28 Mpa for nanoHA/Gel where HA is 10% in weight, and 4.01 MPa with HA being 30% in weight. All the foams showed a similar stress-strain behavior. Even when the brittle HA was added to the gelatin at 30 wt %, the gelatin composite responded efficiently to applied stress, by absorbing energy and dissipating stress without being fractured. Wet state results were not discussed, in attempt to limit the number of variables in that study. Table 1 from the above sited paper show a small change in the elastic modulus values. That is why only dry state was analyzed in this study, in the effort to reduce the amount of variables. Once, dry state study is finalized wet state study will be initiated in a future project.

Table1: Elastic Modulus measured From Compressive Stress-Strain Curves within Initial Stage (<2% Strain).

Foams	Gelatin		10% HA		30% HA	
	Dry	Wet	Dry	Wet	Dry	Wet
Elastic Modulus (MPa)	0.86±0.19	0.63±0.25	2.28±0.10	0.91±0.21	4.01±0.39	1.12±0.15

Also, the published paper of J.Song et al [<sup>2</sup>] showed good mechanical properties for the nanoHA/gel composite. The authors said that the stiffness of the composite and

the ability to withstand compressive stress correlate with the microstructure and content of the mineral component. The incorporation of porous aggregates of HA nanocrystals effectively improved the resistance of the composite to crack propagation under compression. Freeze-dried FlexBone containing 50 wt % porous HA nanocrystals could withstand hundreds-of-megapascals compressive stress and >80% compressive strain without exhibiting brittle fractures.[<sup>3</sup>]

So, the presence of hydroxyapatite in bone is critical to its stiffness. Experiments show a continuous increase in Young's modulus – up to a factor of three for high mineral contents – as collagen fibrils mineralize. [<sup>3</sup>]

## CHAPTER 2

### EXPERIMENTAL METHODS

#### A. Fabrication of scaffolds

In my research, I followed the novel freeze-drying method for the fabrication of my samples. Similar to the work done by J. Liuyun, et al [<sup>31</sup>] the n-HA/gel scaffold was fabricated as described by the following procedure. Firstly, the desired amount of gelatin powder will be added to 30 ml of distilled water (18MΩ.cm) and stirred at 1000 rpm on a temperature about 80 °C until it is well mixed in the water. The quantity of gelatin and Ha particles will depend on how much we need each to be represented in wt % to achieve different types of porosity. Secondly, the desired amount of n-HA solution will be added and the entire solution will be constantly stirred for 3~4 hours under the same conditions to obtain a homogeneous mixture. When the total solution reaches 10 ml in volume, it will be quickly poured into containers with caution that no air bubbles are stuck in there, and then the container got maintained in a freezer at -8°C for overnight to freeze. Finally the sample got lyophilized in a freeze dryer until dried, and a scaffold will be achieved. This procedure is summarized in figure 5.

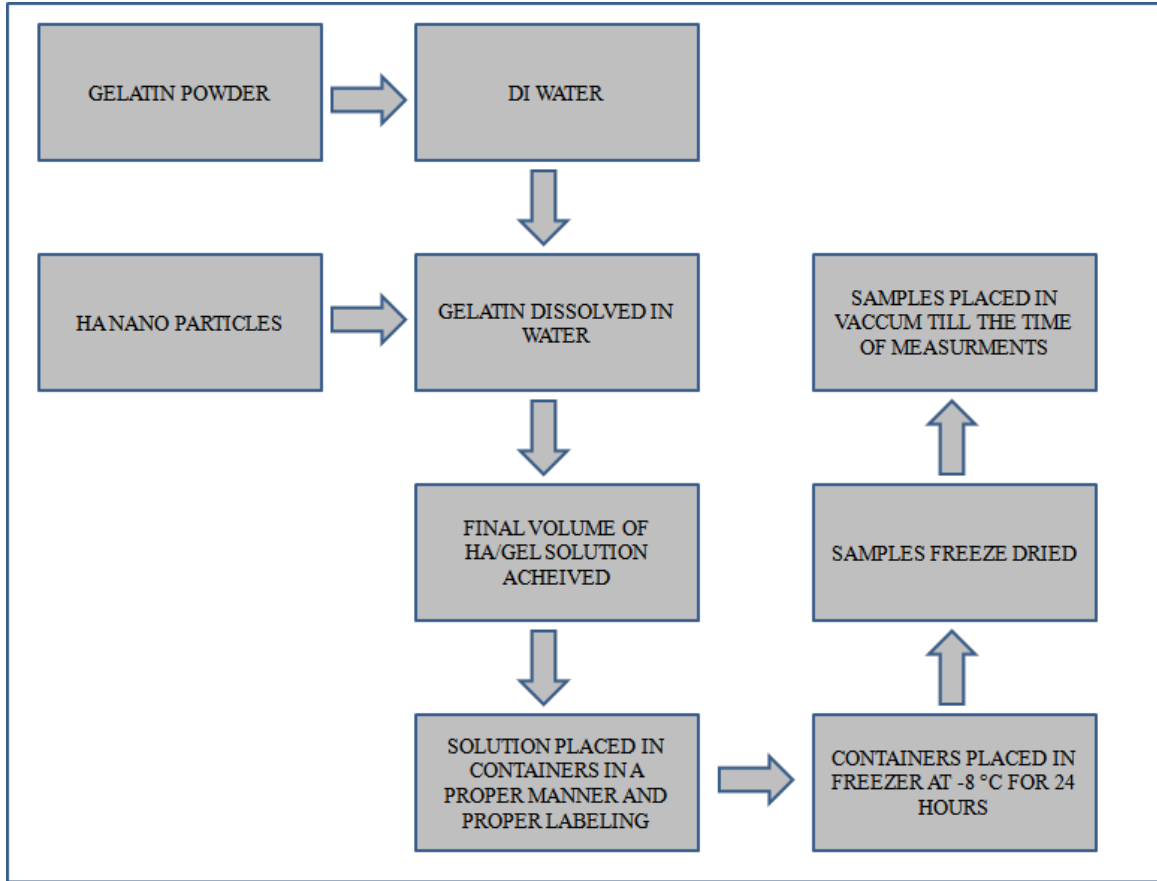


Figure 5: Schematic of synthesis of HA/Gel Scaffolds.

After freeze drying, all samples got labeled and saved in a vacuum environment until time of measurements. Some of the samples were selected for crosslinking procedure. This procedure consisted of immersing the samples in a solution of 8 ml of glutaraldehyde 50 % w/w and 2ml of Methanol for 3 hours. Then samples got well rinsed with methanol. Labeled and placed in vacuum. The density and porosity of the scaffolds were measured by calculating dimension and weight based on the formula:

$$Porosity = 1 - \frac{\rho_s}{\rho_b} \quad (1)$$

Where  $\rho_s$  is the density of the sample and  $\rho_b$  is the density of the bulk material of the sample. And  $\rho_b = \frac{m_1+m_2}{v_1+v_2}$  where  $m_1$ ,  $m_2$ ,  $v_1$ ,  $v_2$  are the mass and the volume of each

composite correspondingly. Volume can be obtained using the specific gravity of each element,  $\rho_{HA} = 3.08 \text{ g/cm}^3$  and  $\rho_{Gel} = 0.7 \text{ g/cm}^3$

The measurements yielded values that varied between 87 % to 90 % porosity  $\pm 1.5$  %.

## B. Method of Investigation

### i. Structural investigation

For structural investigations, SEM images were taken for the samples to facilitate the study of their morphological characteristics like the quality of the interconnections between the pores and the walls of the macropores.[<sup>2</sup>], [<sup>31</sup>] This SEM images were taken at the University of Alabama using their SEM microscope (JEOL 7000 FE SEM that is equipped with EDX, WDS, EBSD, SE, BE and TE detectors, plus Nability E-beam lithography).

In order to illustrate intermolecular interaction between components in the system, to analyze the structure and to study if there is any change in the composition of the particles after compounding. A Fourier Transform Infrared Spectroscopy (FTIR, Vertex 70 spectrometer) were taken to determine the chemical composition of nanoHA/Gelatin composite materials. Using the The FTIR spectra were acquired in transmission mode using the thin (less than 50  $\mu\text{m}$  thick) slices of the fabricated constructs. In all cases, the FTIR spectra represented an average of 100 scans recorded with a resolution of  $4 \text{ cm}^{-1}$  for each sample to reduce the signal/noise ratio.

Then X-ray diffraction (Philips X'pert thin film X-ray diffractometer with  $\text{Cu K}\alpha$  radiation operated at 45 kV and 40 mA, wavelength 0.15406 nm) was used to evaluate the structural characteristics of the prepared nanoHA/gelatin materials in organic and

inorganic phase, and to be able to evaluate the crystalline phases of the HA particles in our samples. [2], [31], [32]. The range was 20 to 50 and  $\theta=15^\circ\text{C}$ .

## ii. Mechanical Testing

The mechanical measurements were made using the Dynamical Mechanical Analyzer “DMA” (DMA 8000, PerkinElmer, Inc.) This instrument will help us determine the Young’s modulus and tension modulus of our samples.

The used DMA is located in the Chemistry department in Dr. Sergey Vyazovkin lab. The testing conditions will be conducted with a dual cantilever, in dry conditions from  $25^\circ\text{C} \sim 40^\circ\text{C}$ ; with a strain factor of 2600N a frequency of 1Hz and displacement of 0.05 mm.

On first stage previously prepared samples, by graduate students who worked before on the project with Dr. Stanishevsky, were measured for tension and bending moduli. Those samples were prepared by the same method described earlier for the preparation of the new samples, which were subject to the same tests as the old ones. All measurements were done using The “DMA” machine mentioned earlier (DMA 8000, PerkinElmer, Inc.). The DMA, Bending test Assembly and Tension Test Assembly are shown in figure 6.

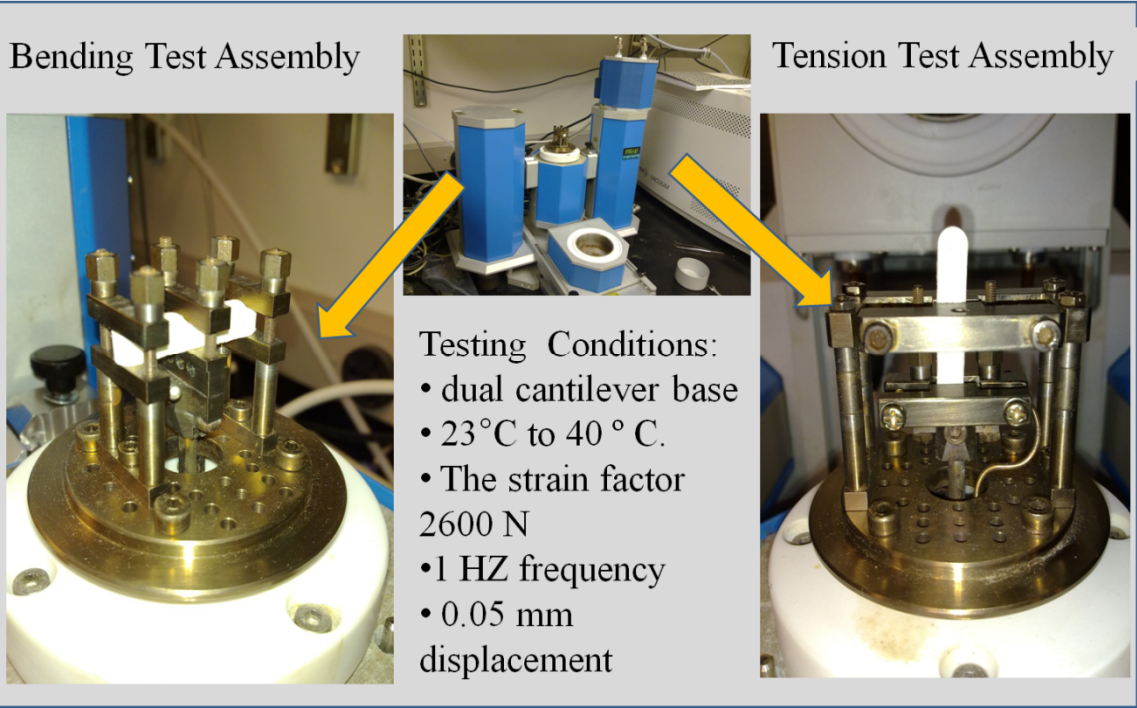


Figure 6: Test assembly for Mechanical testing.

## **CHAPTER 3**

### **RESULTS AND DISCUSSION**

#### **A. SEM RESULTS:**

SEM images were taken from a cross cut of each of the samples. Figure 7 illustrates the test sample and the area where the pictures were taken. The HA addition produced smaller pores and rougher pore wall surfaces. The SEM pictures showed the dimensions of the pores decrease when the inorganic phase content is increased. The HA particles dispersed homogenously in the gel network. [32] All fabricated constructs had three dimensional complicated irregular porous structures with good interconnected porosity up to 90 %, pore diameter in the range of 20 to 300 micron, and pore wall thickness in the range of 3 to 10 micron. Typical SEM images of the samples are shown in Figure 8, 9 and 10.

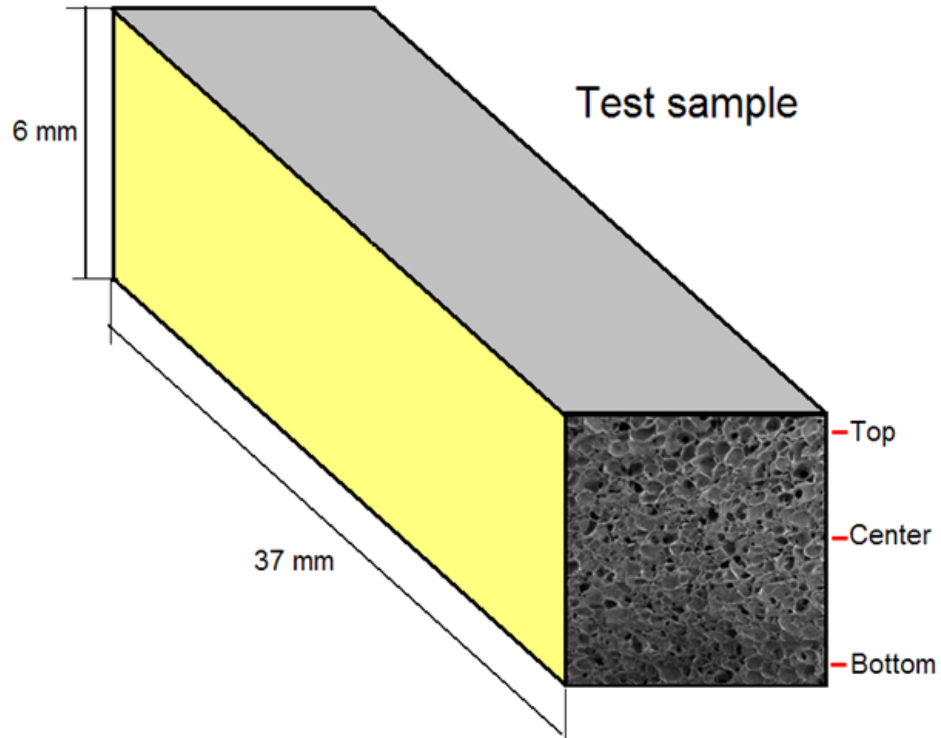


Figure 7: Test sample for SEM images and the areas where the picture were taken.

i. Sample 1: 10% HA by weight:

With the addition of 10 wt% of HA, the pore configuration show a complex morphology. But the general sample was very smooth with big pore size up to 300 microns and much similar to the Gel polymer then a scaffold shape.

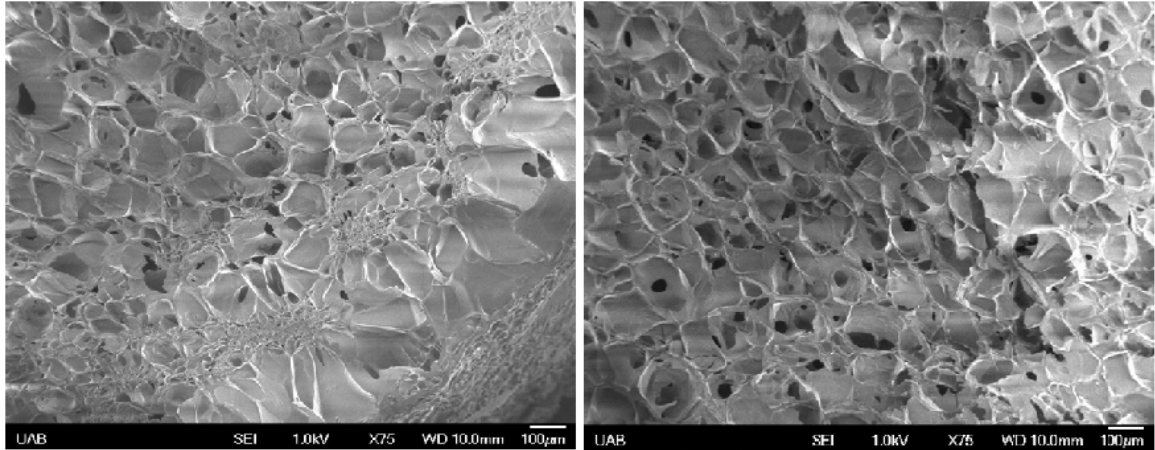


Figure 8: SEM pictures for Sample 1 that contain 10 wt % HA. Left Picture shows the top of the sample, right picture show the center of it.

ii. Sample 2: 30% HA by weight:

On the other hand with 30 wt % HA addition, the pores structure became much complex and anisotropic with irregular pore size from 50 to 90 micron. The walls were rough which what we think it will allow adhesion with cells in the future during implants. The HA particles were distributed homogeneously throughout the gelatin network, and the distribution was not affected by gravity, due to the viscosity of gelatin and rapid freezing of the samples. [23]

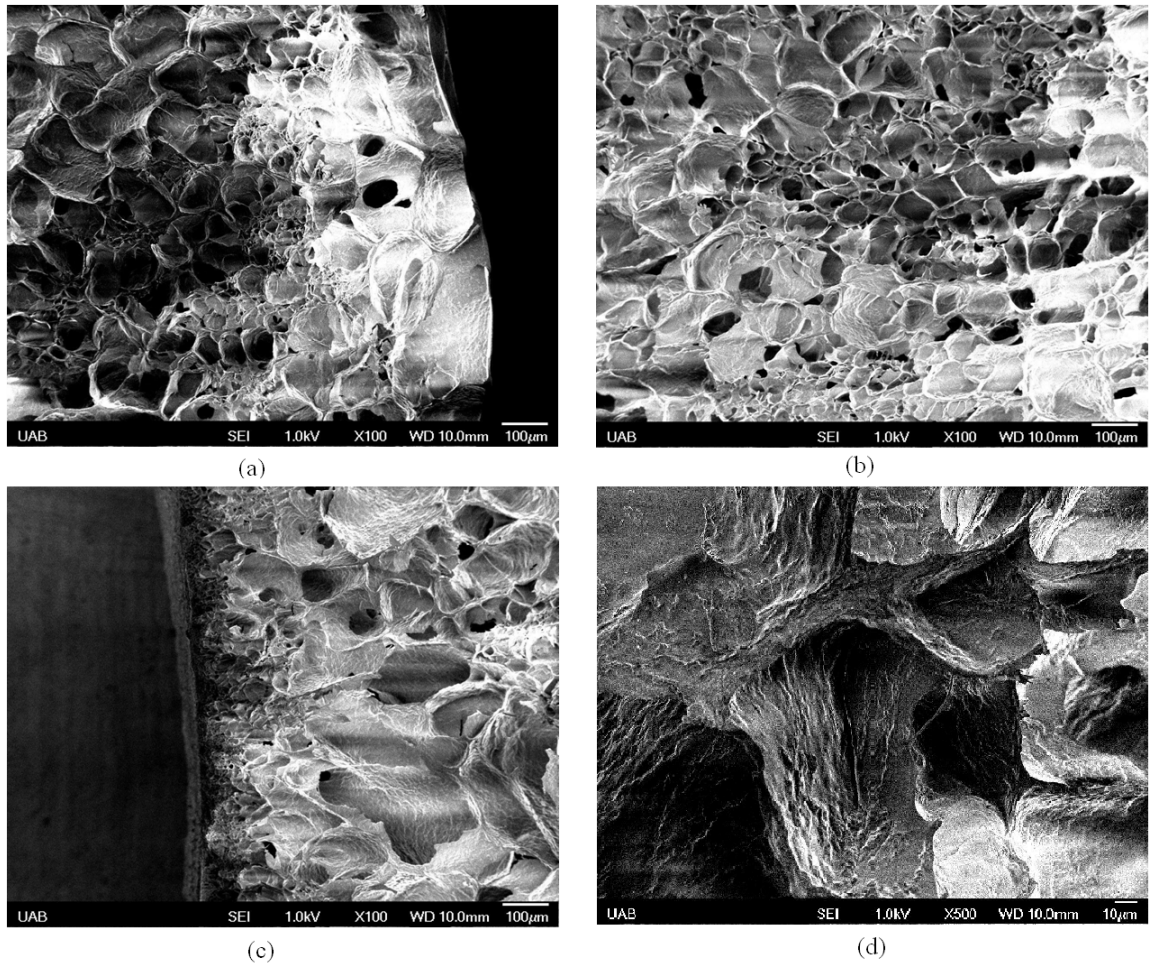


Figure 9: SEM pictures for Sample 2 with 30 wt % HA. (a) Top of the sample x100, (b) Center of the sample x100, (c) Bottom of the sample x100, (d) Center of the sample x 500.

iii. Sample 3: 50% HA by weight:

For the last sample the addition of HA was 50 wt %. The SEM images show a higher irregularity with pore size that drop down to 30 microns. The pore shape became more irregular, and the surface of the walls was much rougher than sample 2, due to the impregnated HA. With this big load of HA, the nanoparticles agglomerated and form aggregates on the surface of the pore walls.

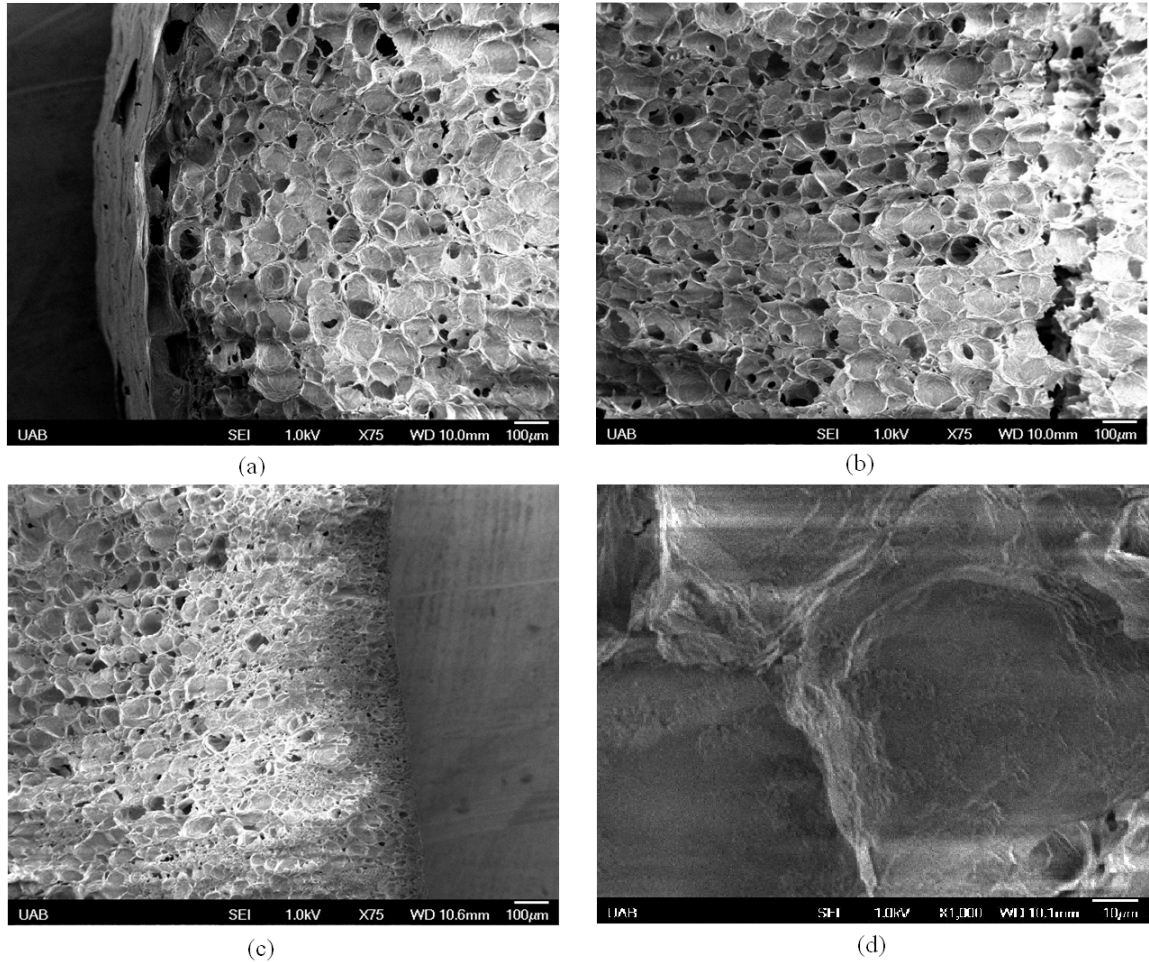


Figure 10: SEM pictures for Sample 3 with 50 wt % HA. (a) Top of the sample x75, (b) Center of the sample x75, (c) Bottom of the sample x75, (d) Center of the sample x 1000 showing the aggregation of the particles on the walls.

#### B. XRD Measurements:

The XRD measurements allowed us to study the crystalline composition of the HA/Gelatin scaffold as shown in figure 11. For pure Gelatin we can notice at  $2\theta \sim 20^\circ$  we have a broad peak that represent the cristanility of the polymer, that was reduced with addition of HA particles. The small peak that appears at  $37.5^\circ$  did not match any other

founding in literature; so, it was contributed as an artifact. On the other hand, when HA was added, diffraction peaks corresponding to HA were observed, and with increasing the HA the intensity of those peaks was increased correspondingly. Those peaks confirmed that HA particles in the samples are of a single-phase apatite. The XRD pattern of the samples containing HA is well matched to the standard HA PDF No#72-1243, and HA particles did not perform a phase change during sample fabrication, since the XRD analysis detected no secondary phases beside HA in scaffolds.[<sup>33</sup>],[<sup>34</sup>],[<sup>26</sup>]

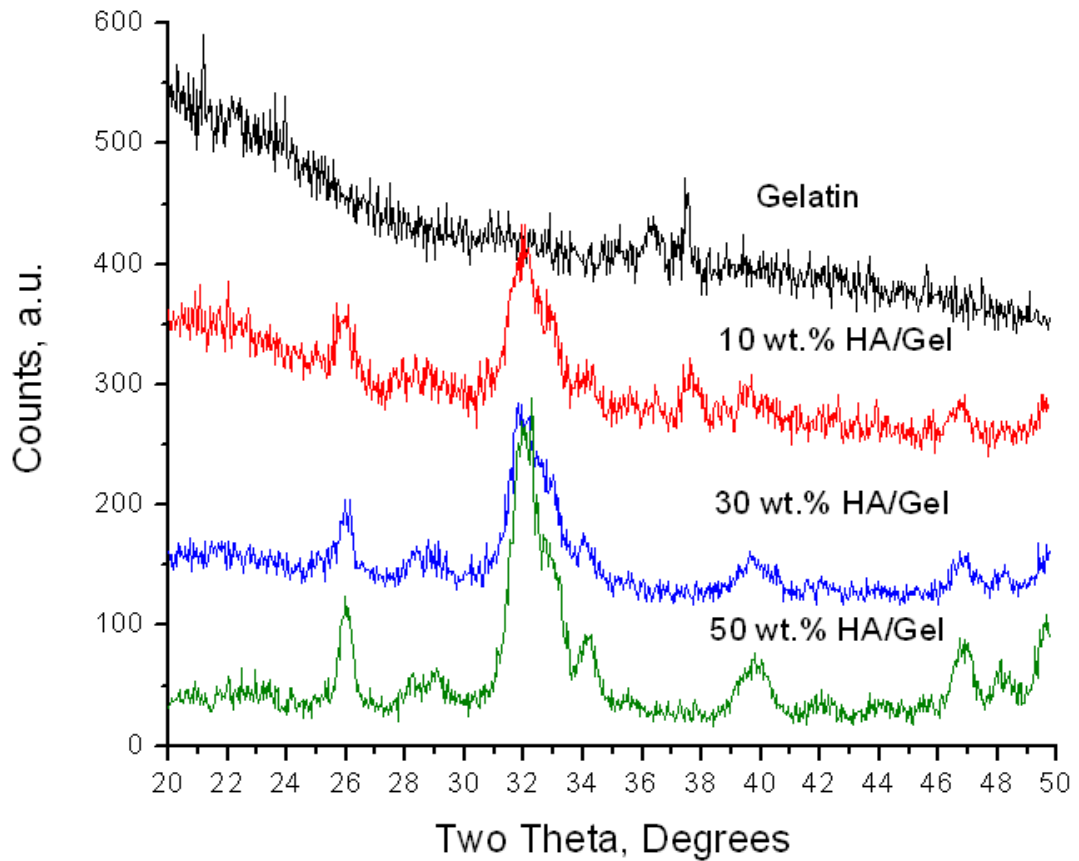


Figure 11: XRD patterns of the gelatin and gelatin-HA composite foams.

Using the Debye-Scherrer equation:  $L_p = \frac{\lambda}{\sqrt{\Delta_{hkl}^2 - \Delta_{Si}^2} \cdot \cos \theta}$ , the size of the used HA particles was determined to be  $L_p = \frac{1.5406 \cdot 10^{-10}}{\sqrt{(99 \cdot 10^{-4})^2 - (0.29 \cdot 10^{-4})^2} \cdot \cos 13} = 16nm$ .

Where  $\lambda$  is the wave length of the X-ray,  $\Delta_{hkl}$  and  $\Delta_{Si}$  are the full width at half maximum (FWHM) for the peak at  $\theta = 13^\circ$  and for Silicon, respectively.

### C. Infrared Spectroscopy:

IR spectroscopy of pure gelatin revealed a series of amide ( $1240 \text{ cm}^{-1}$ ,  $1540 \text{ cm}^{-1}$ , and  $1650 \text{ cm}^{-1}$ ) and carboxyl ( $1300\text{-}1450 \text{ cm}^{-1}$ ) bands, which were attributed to the amino acids of gelatin backbone, such as glycine, proline, and hydroxyproline. [35] After adding HA,  $\text{PO}_4$  ( $570 \text{ cm}^{-1}$ ,  $600 \text{ cm}^{-1}$ ,  $960 \text{ cm}^{-1}$ , and  $1030\text{-}1090 \text{ cm}^{-1}$ ) bands appeared clearly along with gelatin bands. [36], [37] The increase in HA amount increased the intensity of  $\text{PO}_4$  and decreased the one corresponding to gelatin. No significant change was observed in band structure of gelatin with the addition of HA nanoparticles, which confirmed that no chemical reaction, occurred between HA and gelatin in the composites.

Figure 13 shows the FTIR spectra of the same samples as in figure 12, but after crosslinking. The results show that the bands of gelatin are much conserved with the addition of HA, while the HA bands were not affected that much. Prove that gelatin retained considerable biological characteristic groups, especially amino acids. Moreover, the evolution of amide bands suggested that the gelatin maintained a high level of the unique sequence of  $\alpha$ -helical structure.[38]

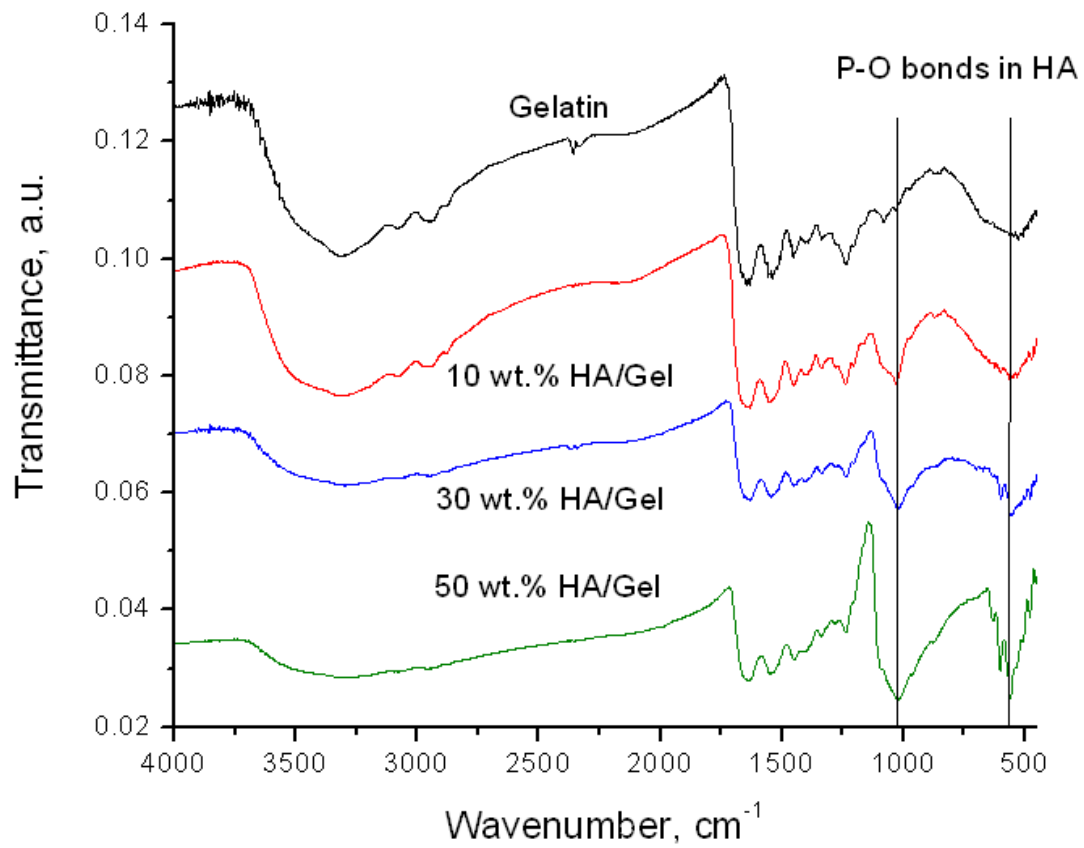


Figure 12: IR spectra for gelatin sample, and all other samples before Crosslinking.

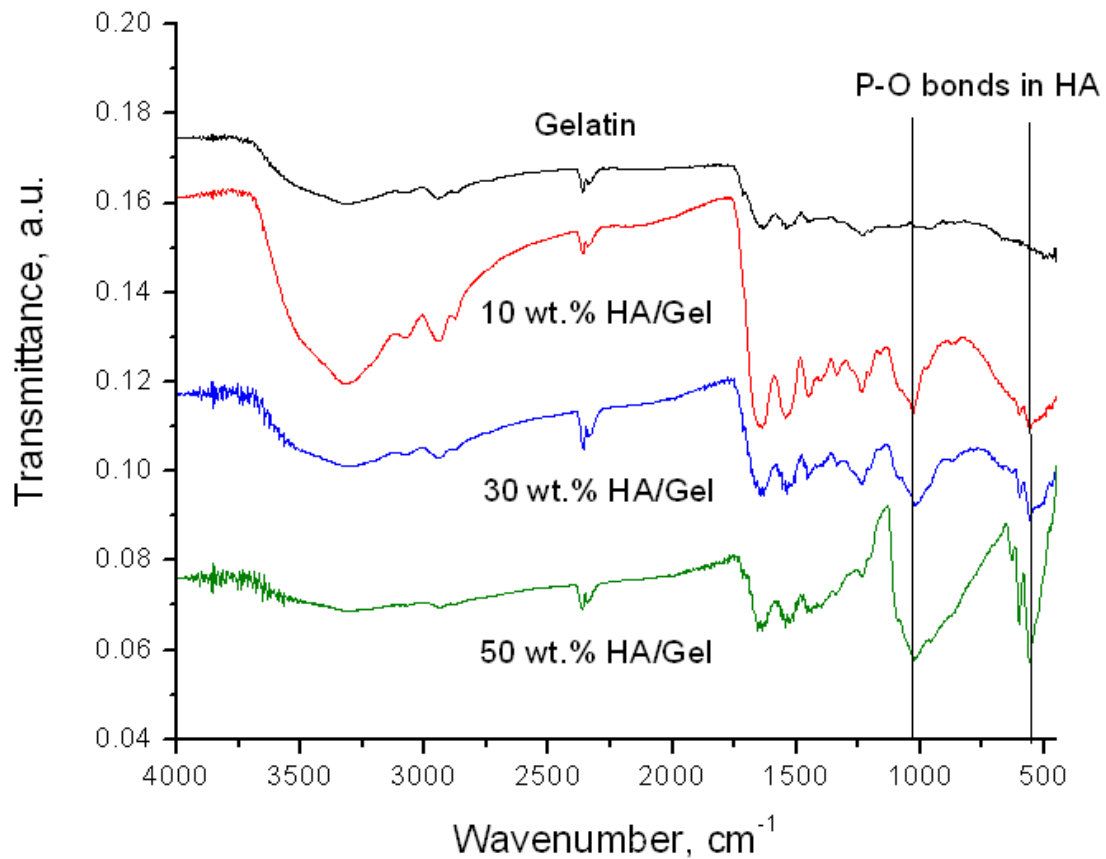


Figure 13: IR spectra for gelatin sample, and all other samples after Crosslinking.

#### D. Mechanical Testing:

Pure gelatin sample were prepared and their mechanical properties were measured for the purpose of comparison. Their dynamic mechanical analysis (DMA) revealed a bending modulus about 2.5 GPa and a tension modulus about 2 GPa before crosslinking.

After Crosslinking, the average of the bending modulus grows in a factor of 3 at least to become 5.5 GPa and the tension modulus became 2.3 GPa.

DMA study of previously prepared nanoHA/Gel scaffolds, sample batch 1, revealed the bending (Fig 14) and tensile moduli (Fig 15) up to 500 MPa and 800 MPa,

respectively, when nanoHA loading was around 30 % by weight. These moduli increase by a factor of 1.6 after the cross-linking of polymer (Fig 16 and 17). NanoHA loading above 50 % by weight results in both moduli above 2 GPa (Fig 14 and 15), but the cross-linking reduces them significantly (Fig 16 and 17). There was another samples prepared with a different type of nanoHA particles, called Type 2. These samples showed very low moduli for bending and tension less than 8 MPa, and they got even lower after crosslinking. So, they got eliminated from the study due to their brittleness and incapability of achieving the desired scaffold.

So far, it has been further shown that the uniform dispersion of nanoHA within the polymer matrix improves the mechanical properties of the scaffolds. As well as corsslinking, in the case of such dispersion. And since HA is a brittle compound, over loading of it, such in the case of 50 wt% load, contribute in a lower bending modulus then 30 wt % loading. What suggest the liability of sample 2 containing 30 wt % on achieving the desired mechanical properties of the scaffolds in question.

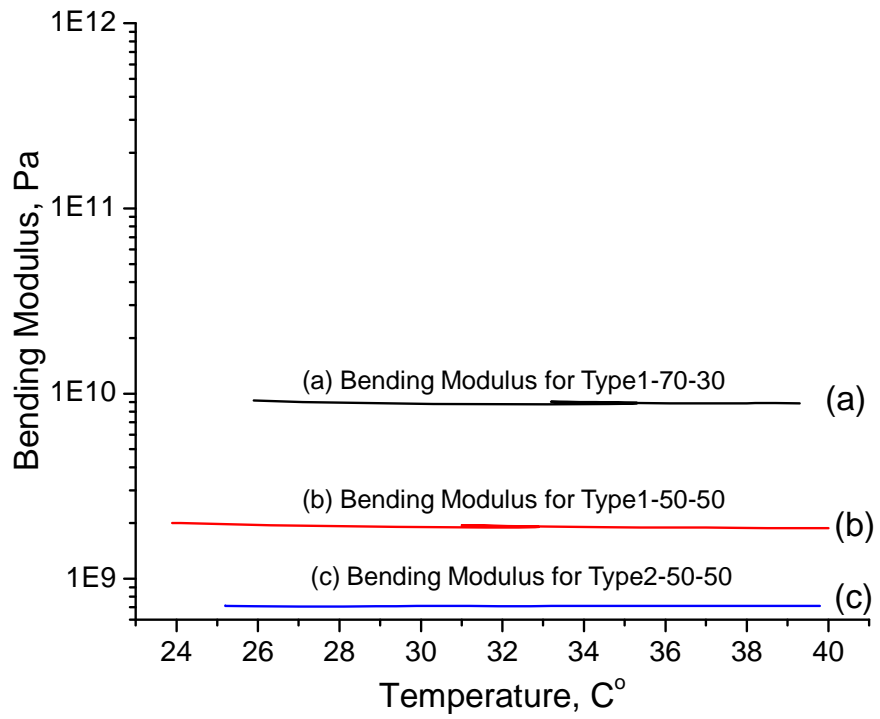


Figure 14: Comparison for bending modulus between all batch 1 samples before crosslinking.

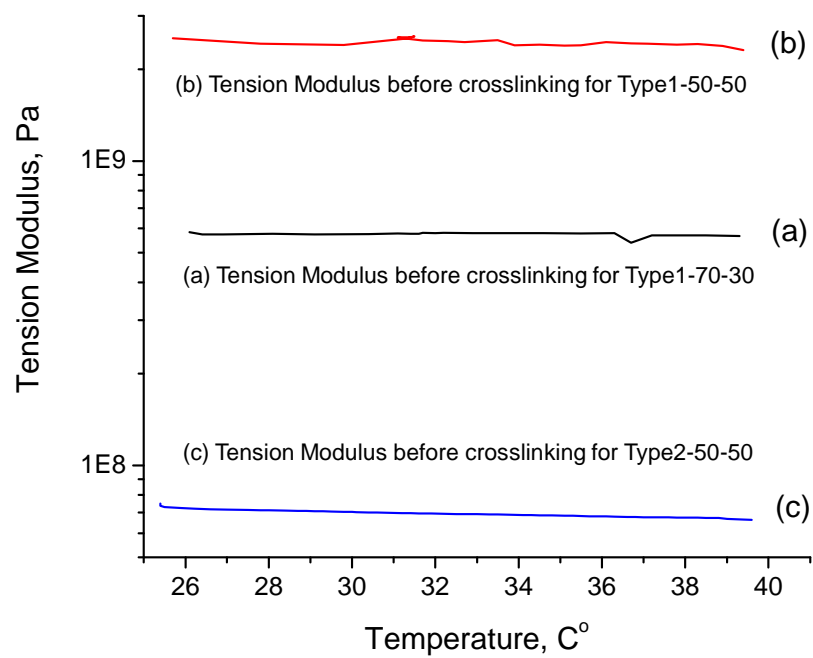


Figure 15: Comparison for tension modulus between all batch 1 samples before crosslinking.

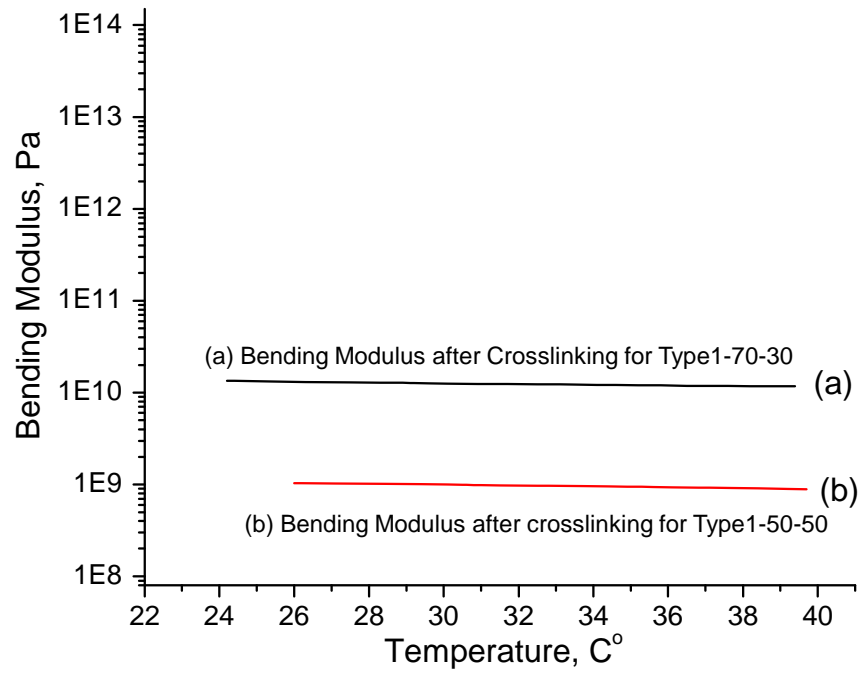


Figure 16: Comparison for bending modulus between all batch 1 samples after crosslinking.

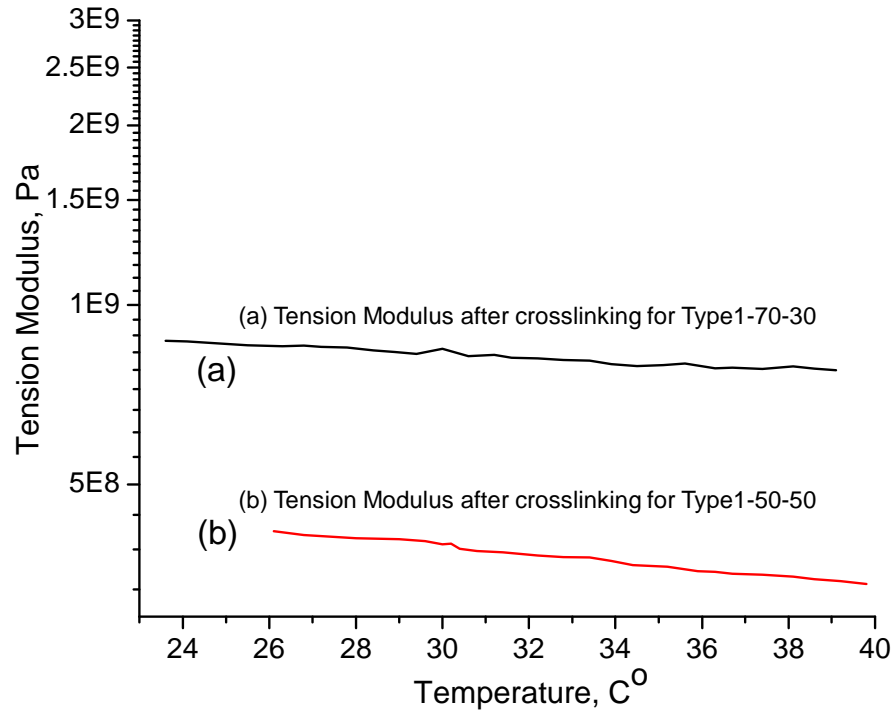


Figure 17: Comparison for tension modulus between all batch 1 samples after crosslinking.

For the new prepared samples, so called batch 2 samples, dynamic mechanical analysis (DMA) revealed the bending (Fig 18) and tensile moduli (Fig 19) up to 2.3 GPa and 1.2 GPa, respectively, when nanoHA loading was around 10 % by weight. After crosslinking these moduli went up to 4 GPa and 3 GPa respectively. For 30 wt % load of HA bending and tensile moduli were up to 1.28 GPa and 1.5 GPa, respectively. The bending modulus increase by a factor of 1.6 after the cross-linking of polymer (Fig 20). While the tension drop to about 150 MPa. NanoHA loading above 50 % by weight results in bending modulus about 700 MPa and Tension modulus about 200 MPa (Fig 18 and 19), the cross-linking enhanced the bending up to 1 GPa while it did not affect much the Tension (Fig 20 and 21).

So far, it has been shown again that the uniform dispersion of nanoHA within the polymer matrix improves the mechanical properties of the scaffolds. As well as crosslinking, in the case of such dispersion. And similar to batch 1 samples, sample 3 (50 wt %) show brittleness, while sample 1 (10 wt %) and sample 2 (30 wt %) showed good bending and tension moduli.

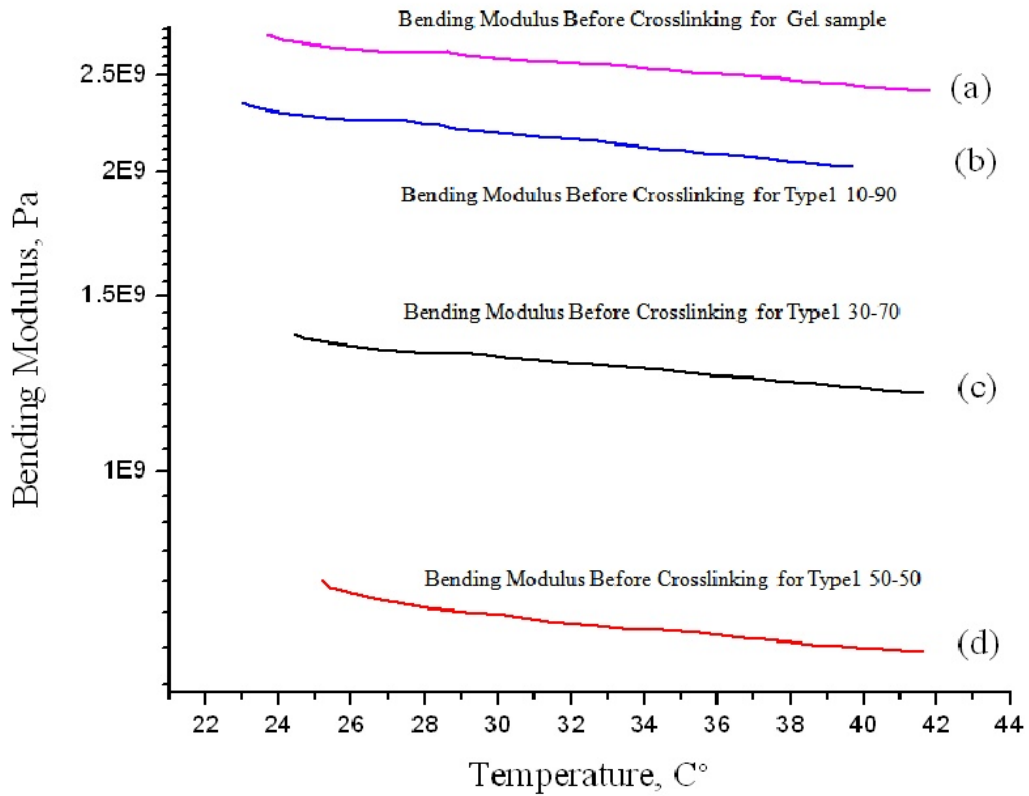


Figure 18: Comparison between the Bending Modulus of all new samples before Crosslinking.

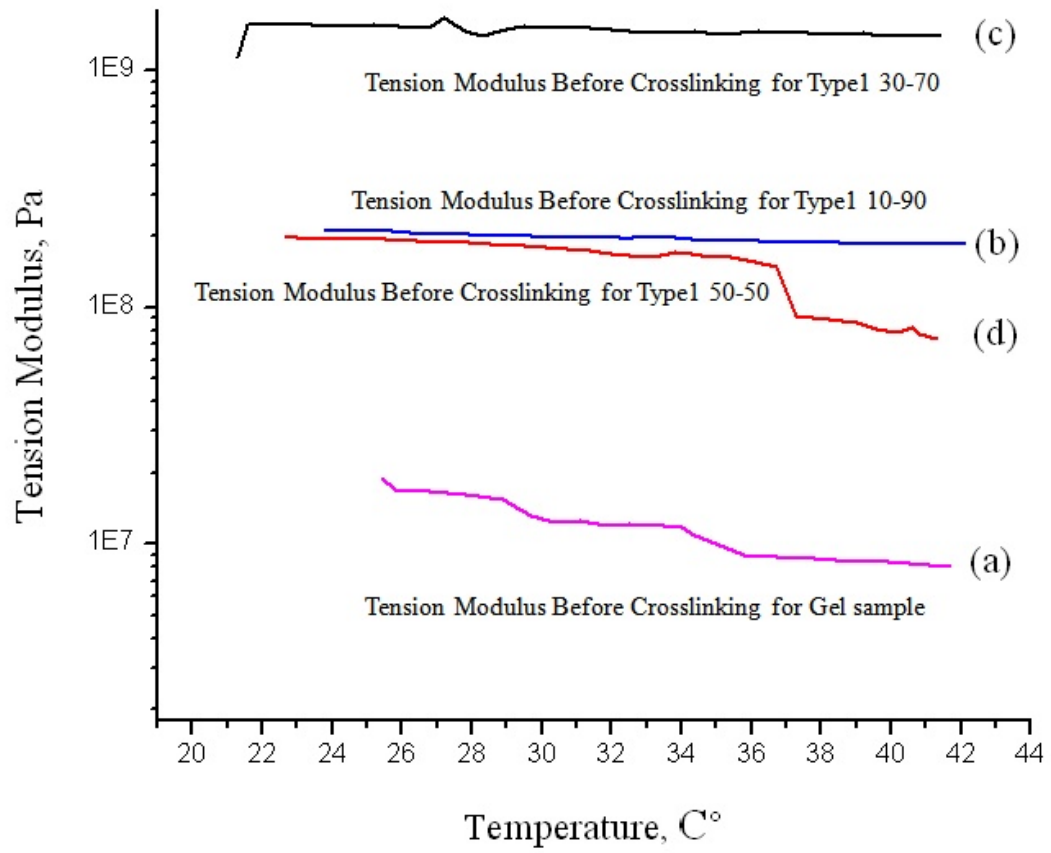


Figure 19: Comparison between the Tension Modulus of all new samples before Crosslinking.

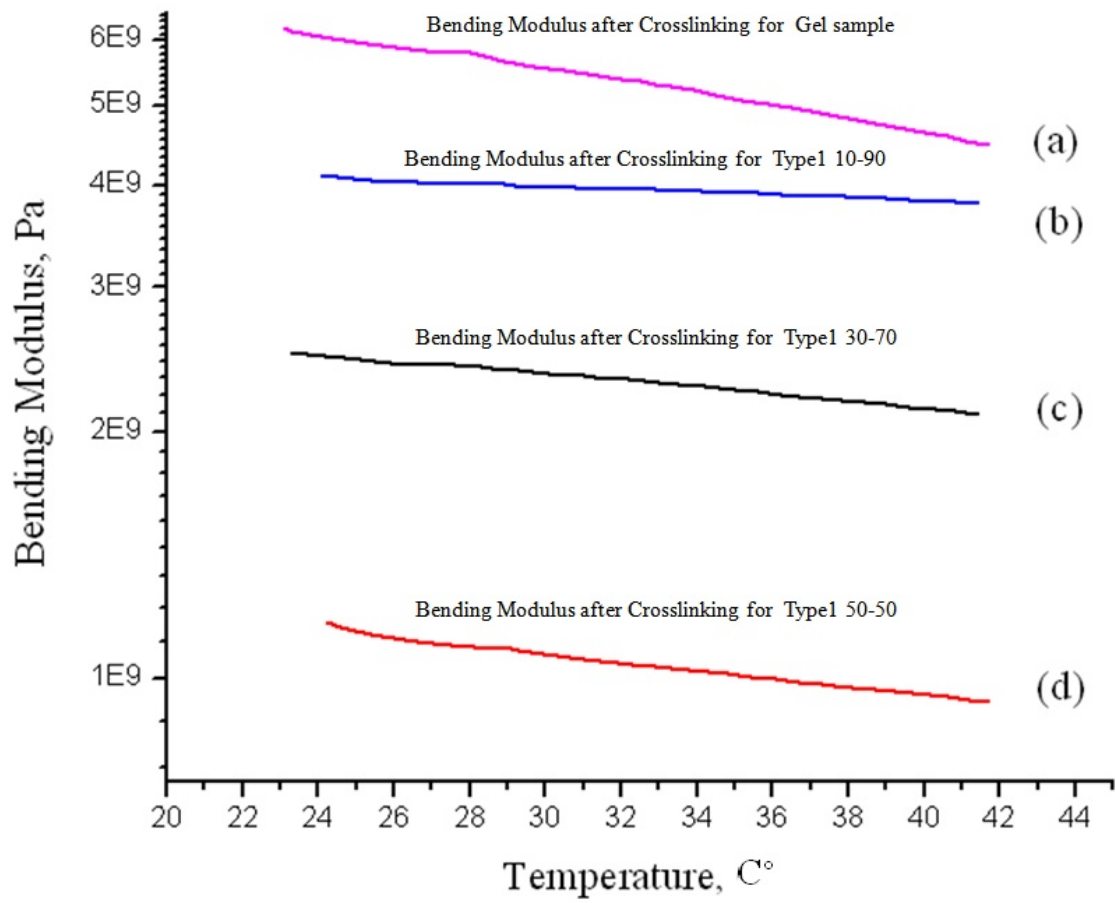


Figure 20: Comparison between the Bending Modulus of all new samples after Crosslinking.

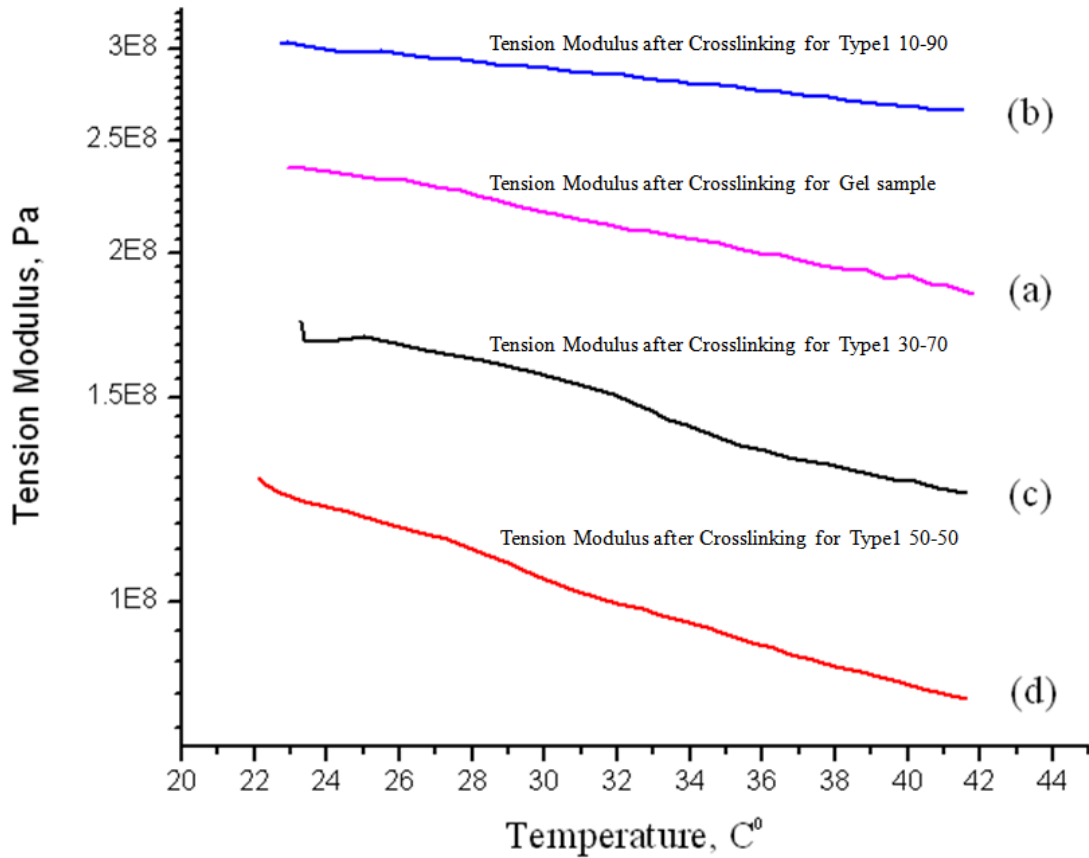


Figure 21: Comparison between the Tension Modulus of all new samples after Crosslinking.

The mechanical studies showed that the tension and bending moduli were affected by the ratio of HA particles to quantity of gel in the sample, due to the brittleness of the HA particles. As well by crosslinking that improves the mechanical properties of the scaffolds. And since the sample were tested in dry condition, it is expected that all moduli will drop a little bit in wet condition as shown by the study done in sited paper [26] and table1. This drop will make our moduli meet the human bone moduli or be a little higher for better performance. As a reference, the peak contact stresses in natural human joints

during light to moderate activity typically range from 0.5-6 MPa by most *in vitro* measurements<sup>[39][40]</sup> and up to 18 MPa by some *in vitro* measurements.<sup>[41][42]</sup>

We can say as well for all samples that the stress-strain behavior was the same; small increment at the beginning then undergoes a constant small reduction in slope. Such behavior is usually observed in polymers that undergo considerable plastic deformation <sup>[43], [44]</sup>. The gelatin did not show a final fracture; even with the addition of the brittle HA up to 50 wt %. The weird loop that appeared in the bending graph for the batch 1 samples did not occurred in the graph of the crosslinked samples neither in the bending graph for the batch 2 samples. This weird result was not mentioned in any of the data before, and the suggested scientific explanation, is to contribute this phenomenon to the crystallization of polymer at that specific temperature.

As a summary, Gelatin / Hydroxyapatite (HA) composites were fabricated in a porous structure through a novel combination of mixing, freeze-drying and cross-linking processes. The followed method allowed the preparation of composite scaffolds with tailored composition and porous microstructure, with good porosity that based on literature will meet the basic requirement to grow for new bone tissue and cell adhesion in future implant application. Since it has been demonstrated <sup>[45]</sup> that human cells proliferate well on gelatin scaffolds with anisotropic channel-like porosity, similarly to on corresponding isotropic scaffolds of the same porosity. And as demonstrated by the result only sample 1 and 2 were close in their moduli to those of human bone, but sample 1 (10 wt % load of HA) was dropped due to its morphological and structural result that did not show the desired porous structure and porous network connectivity between the pores.

## CONCLUSIONS

### Structural and Morphological Studies:

- Freeze drying is a successful method to achieve porosity up to 90 % with pore diameter in the range of 20 to 300 micron, and pore wall thickness in the range of 3 to 10 micron..
- 30 wt % load of HA gave the best pore size up to 30 micron and porous interconnectivity. According to literature such pore size should facilitate cell adhesion and biointegration in the future.
- No phase change in the crystalline phase during processing, and preservation of strong P-O bonds in the HA particles.
- Crosslinking had little effect on the structure and morphology of the polymer and it did strengthen them mechanically.

### Mechanical Studies:

- Tension and Bending moduli are affected by the ratio of HA particles in the sample. Due to the brittleness of the HA particle30 wt % load of HA gave the closest moduli in the range of the human bone.
- Crosslinking affect the mechanical properties of these composites depending on the content of HA. For example it strengthen the moduli in samples with 30 wt % HA, while it reduce them in samples with over 50 wt % HA.

## LIST OF REFERENCES

- 
- <sup>1</sup> M. Wang, Composite Scaffolds for Bone Tissue Engineering, *Amer. J. Biochem. Biotechnol.* **2**, 80-84 (2006).
- <sup>2</sup> J.Song *et al.*, Elastometric high-mineral content hydrogel-hydroxyapatite composites for orthopedic applications, Received 4 April 2008; accepted 8 April 2008. Published online 10 June 2008 in Wiley InterScience. DOI: 10.1002/jbm.a.32110.
- <sup>3</sup> R. O. Ritchie *et al.*, Plasticity and Toughness in Bone, *Physics Today* June p.41. (2009)
- <sup>4</sup> J.R. Woodard *et al.*, The Mechanical properties and osteoconductivity of hydroxyapatite bone scaffolds with multi-scale porosity, *ScienceDirect Biomaterials* **28** 45-54. (2007)
- <sup>5</sup> AG Word *et al.*, *The science and Technology of gelatin*, London: Academic Press (1977).
- <sup>6</sup> Gibson LJ *et al.* *Cellular Solids: Structure and Properties*, Cambridge University Press, Cambridge (1997).
- <sup>7</sup> Wang M, Developing bioactive composite materials for tissue replacement, *Biomaterials*, **24**: 2133-2151, (2003).
- <sup>8</sup> Hench L.L. *J Am, Bioceramics: from concept to clinic*, *Ceram Soc* **74**:1485-1510, (1991)
- <sup>9</sup> Brown PW *et al.* ,*Hydroxyapatite and related materials*, London: CRC Press; (1994).
- <sup>10</sup> Silvio L *et al.* , Biodegradable drug delivery system for the treatment of bone infection and repair, *J Mater Sci Mater Med*;**10**:653-658. (1999)
- <sup>11</sup> Tampieri A *et al.* ,Porous phosphate gelatin composite as bone graft with drug delivery function, *J. Mater Sci. Mat Med*;**14**:623-7, (2003).

- 
- <sup>12</sup> Liu B *et al.*, Porous bioceramics reinforced by coating gelatin, *J Mater Sci: Mater Med.* DOI **10.1007/s10856-007-3216-1**.
- <sup>13</sup> E.Landi *et al.*, Porous hydroxyapatite/gelatin scaffolds with ice-designed channel-like porosity for biomedical applications, Available online at [www.sciencedirect.com](http://www.sciencedirect.com) *Acta biomaterialia* **4** 1620-1626. (2008)
- <sup>14</sup> Otani Y *et al.*, Effect of additives on gelation and tissue adhesion of gelatin-poly (L-glumatic acid) mixture, *Biomaterials*; **19**:2167-2173. (1998)
- <sup>15</sup> Kimura Y, Biomedical applications in polymeric materials, Biodegradable polymers In: Tusruta T, editors. Boca Raton, FL: CRC Press;. P **163** (1993)
- <sup>16</sup> D.-A. Wang *et al.*, Multifunctional chondroitin sulphate for cartilage tissue–biomaterial integration, *Nature Mater.* **6** (2007), p. 385.
- <sup>17</sup> C. Wang *et al.*, A novel gellan gel-based microcarrier for anchorage-dependent cell delivery, *Acta Biomater.* **4**, p. 1226. (2008)
- <sup>18</sup> D.-A. Wang *et al.*, Bioresponsive phosphoester hydrogels for bone tissue engineering. *Tissue Eng.* **11**, p. 201. (2005)
- <sup>19</sup> D.-A. Wang *et al.*, Enhancing the Tissue-Biomaterial Interface: Tissue-Initiated Integration of Biomaterials *Adv. Funct. Mater.* **14** (2004), p. 1152.
- <sup>20</sup> Q. Li *et al.*, Heterogeneous-phase reaction of glycidyl methacrylate and chondroitin sulfate: mechanism of ring-opening-transesterification competition, *Macromolecules* **36** p. 2556. (2003),
- <sup>21</sup> C. Wang *et al.*, The control of anchorage-dependent cell behavior within a hydrogel/microcarrier system in an osteogenic model. *Biomaterials* **30**, p. 2259. (2009)

- 
- <sup>22</sup> Y. Gong *et al.*, *In vitro* and *in vivo* degradability and cytocompatibility of poly(l-lactic acid) scaffold fabricated by a gelatin particle leaching method. *Acta Biomater.* **3**, p. 531. (2007)
- <sup>23</sup> D.-A. Wang *et al.*, Synthesis and characterization of a novel degradable phosphate-containing hydrogel, *Biomaterials* **24**, 3969.
- <sup>24</sup> Y. Hong *et al.*, Small diameter, fibrous vascular conduit generated from a poly(ester urethane)urea and phospholipid polymer blend. *Biomaterials* **30** (2009), p. 2457.
- <sup>25</sup> M. Borden *et al.*, Tissue Engineered microsphere-based matrix for bone repair: design and evaluation. *Biomaterials* **23** p. 551. (2002),
- <sup>26</sup> H.w. Kim *et al.*, Hydroxyapatite and gelatin composite foams processed via novel freeze-drying and crosslinking for use as temporary hard tissue scaffolds, [www.interscience.wiley.com](http://www.interscience.wiley.com). DOI: **10.1002/jbm.a.30168**
- <sup>27</sup> J.D. Currey, What Determine the Bending Strength of Compact Bone? , *The Journal of Experimental Biology* **202**, 2495-2503 (1999) printed in great Britain © The Company of Biologists Limited 1999 JEB 1959.
- <sup>28</sup> Wang M *et al.*, Manufacture and evaluation of bioactive and biodegradable materials and scaffolds for tissue engineering,. *J Mater Sci: Mater Med*, **12**: 855-860(2001)
- <sup>29</sup> Weng J *et al.*, Producing chitin scaffolds with controlled pore size and interconnectivity for tissue engineering,. *J Mater Sci Lett*, **20**: 1401-1403 (2001)
- <sup>30</sup> Sultana N *et al.*, Fabrication and characterisation of polymer and composite scaffolds based on polyhydroxybutyrate and polyhydroxybutyrate-co-hydroxyvalerate, *Key Engineering Materials*, (2006)

- 
- <sup>31</sup> J. Liuyun *et al.*, Preparation and biological properties of a novel composite scaffold of nano-hydroxyapatite/chitosan/carboxymethyl cellulose for bone tissue engineering, Published: 14 July 2009, Received: 31 October 2008, Accepted: 14 July 2009. *Journal of Biomedical Science*, **16**:65 doi:10.1186/1423-0127-16-65. (2009) This article is available from: <http://www.jbiomedsci.com/content/16/1/65> © 2009 Liuyun et al; licensee BioMed Central Ltd.
- <sup>32</sup> S. Panzavolta *et al.*, Porous composite scaffolds based on gelatin and partially hydrolyzed  $\alpha$ -tricalcium phosphate, Available online at [www.elsevier.com/locate/actabiomat](http://www.elsevier.com/locate/actabiomat) *Acta Biomaterialia* **5** 636-643, (2009).
- <sup>33</sup> D. Wang *et al.*, Fabrication of superparamagnetic hydroxyapatite with highly ordered three-dimensional pores, Published online: 29 May 2009. *J Mater Sci* **44**:4020-4025 (2009) DOI 10.1007/s10853-00903555-z.
- <sup>34</sup> E.S. Thian *et al.*, Silicon-substituted hydroxyapatite (SiHA): A novel calcium phosphate coating for biomedical applications. *J MATER SCI* **41**:709-717, (2006).
- <sup>35</sup> Word AG *et al.*, The science and technology of gelatin. London: Academic Press; (1977).
- <sup>36</sup> Elliot JC. , *Studies in inorganic Chemistry 18: Structure and chemistry of the apatites and other calcium orthophosphates*. Amsterdam: Elsevier; (1994).
- <sup>37</sup> E. Park *et al.*, Characterization of Hydroxyapatite: Before and after plasma spraying. *Journal of Materials Science: Materials in Medicine* **13** 211-218, (2002).
- <sup>38</sup> K. AW, Chemical modification of the side chains of gelatin. *Biochem J*; **68**:458-468. (1958)

- 
- <sup>39</sup> Ahmed AM *et al.*, In vitro measurement of static pressure distribution in synovial joints-part I: Tibial surface of the knee. *J Biomech Eng*; **105**:216-225. (1983)
- <sup>40</sup> Brand RA. Joint contact stress: A reasonable surrogate for biological processes? *Iowa Orthop J*; **25**:82-94. (2005)
- <sup>41</sup> Hodge WA *et al.*, Contact pressures in the human hip joint measured in vivo. *Proc Natl Acad Sci USA*; **83**:2879-2883. (1986)
- <sup>42</sup> Hodge WA *et al.*, Mann RW, Contact pressures from an instrumented hip endoprosthesis. *J Bone Joint Surg Am*; **71**:1378-1386. (1989)
- <sup>43</sup> Ashby MF *et al.*, Cellular Design guide. Cambridge: Cambridge University Press; (1998).
- <sup>44</sup> Lim TJ *et al.*, Behavior of a random hollow sphere metal foam. *Acta Mater*; **50**:2867-2879. (2002)
- <sup>45</sup> Dubuel P *et al.*, Porous gelatin hydrogels: 2. In vitro cell interaction study. *Biomacromolecules*; **8**: 338-44. (2007)